J Fluoresc (2015) 25:319–325
DOI 10.1007/s10895-015-1511-7

ORIGINAL PAPER

A Dansyl-Rhodamine Ratiometric Fluorescent Probe for Hg^{2+} Based on FRET Mechanism

Puhui Xie · Fengqi Guo · Lingyu Wang · Sen Yang · Denghui Yao · Guoyu Yang

Received: 6 October 2014 / Accepted: 4 January 2015 / Published online: 18 January 2015

Abstract Based on resonance energy transfer (FRET) from dansyl to rhodamine 101, a new fluorescent probe (compound **1**) containing rhodamine 101 and a dansyl unit was synthesized for detecting Hg^{2+} through ratiometric sensing in DMSO aqueous solutions. This probe shows a fast, reversible and selective response toward Hg^{2+} in a wide pH range. Hg^{2+} induced ring-opening reactions of the spirolactam rhodamine moiety of **1**, leading to the formation of fluorescent derivatives that can serve as the FRET acceptors. Very large stokes shift (220 nm) was observed in this case. About 97-fold increase in fluorescence intensity ratio was observed upon its binding with Hg^{2+}.

Keywords Fluorescent probe · Ratiometric · Rhodamine · Dansyl fluorophore · Hg^{2+}

Introduction

Development of highly sensitive probes for target cations has been a significant research area in the field of chemical sensors due to their importance in biological and environmental processes [1–4]. For example, mercury is one of the most hazardous and ubiquitous pollutants [5–7]. Mercury bioaccumulation can involve inorganic mercury and methylmercury species (CH_3HgX), which enter the food chain and are subsequently ingested by humans. Neurological problems associated with methylmercury intoxication include prenatal brain damage, cognitive and motion disorders, vision and hearing loss, and death [8–10].

Therefore, development of sensitive and selective chemosensors for Hg^{2+} in various media is of considerable importance. Fluorimetric sensing is a preferable approach for detection of metal ions or other analytes because fluorimetry is rapidly performed, nondestructive, highly sensitive and suitable for high-throughput screening applications [11–14]. However, Hg^{2+} can quench the luminescence of a fluorophore due to effective spin−orbit coupling mechanism, bound to the receptor functionality of a sensor, and this accounts for the most fluorescence off/quenching-based sensors [15]. Hg^{2+} ions are known to be extensively solvated in an aqueous medium, and the unfavorably high enthalpy of solvation poses a challenge to chemists in developing a suitable receptor for sensing of Hg^{2+} ions in an aqueous environment.

Rhodamine-based probes can resolve the problems of the fluorescence-quenching effect caused by metal ion binding. Rhodamine derivatives with the spirolactam form are colorless (weak absorption) and nonfluorescent, whereas the ring-opened amide form induced by the analyte gives rise to an appearance of pink color (strong absorption) and a strong fluorescence emission at a relatively long wavelength. So the rhodamine framework is an ideal model to design the turn-on fluorescent probe, and many probes for Hg^{2+} have been proposed [16–26]. As reported, the "off-on" fluorescence enhancement in the spectral region of 550–590 nm for these probes is based on the mechanism involving the formation of a ring-opened form from the spirolactam upon cation binding.

Electronic supplementary material The online version of this article (doi:10.1007/s10895-015-1511-7) contains supplementary material, which is available to authorized users.

P. Xie (✉) · S. Yang · G. Yang
College of Sciences, Henan Agricultural University, Zhengzhou 450002, People's Republic of China
e-mail: phxie2013@163.com

F. Guo (✉) · L. Wang · D. Yao
College of Chemistry and Molecular Engineering, Zhengzhou University, Zhengzhou 450001, People's Republic of China
e-mail: fqguo@zzu.edu.cn

However, as the single emission intensity change is the only detection signal, such probes tend to be affected by a variety of factors such as instrumental efficiency, environmental conditions, and probe molecule concentration [27], the simultaneous recording of the fluorescence intensities at two wavelengths and then calculation of their ratio is one of the attractive approaches and provides a built-in correction to eliminate most or all of the ambiguities [28]. The usage of guest-induced fluorescence resonance energy transfer (FRET) mechanism should be one efficient approach to design ratiometric fluorescence probes, since they can emit at two different wavelengths at a single excitation source [29]. For ratiometric fluorescence probes based on the FRET mechanism, the emission of the donor at relative short wavelength induces emission of the acceptor at longer wavelength with their ratio modulated by the guest [30, 31]. In addition, because the pseudo-Stokes shifts of FRET based probes are larger than the Stokes shifts of either the donor or acceptor dyes, the possible self-quenching as well as fluorescence detection errors due to backscattering effects from the excitation source will be efficiently avoided [32]. Up until now, few ratiometric fluorescence probes of rhodamine derivatives for Hg^{2+} based on FRET are developed [33–39].

Herein, a new dansyl-appended rhodamine 101 (compound **1**) based FRET fluorescence probe is developed as a ratiometric Hg^{2+} sensor. A leuco-rhodamine derivative with unconjugated structures as fluorogenic and chromogenic sensors was chosen as a sensitive chemosensor for Hg^{2+} ions. A highly efficient ring-opening reaction induced by Hg^{2+} generates the long-wavelength rhodamine fluorophore which can act as the energy acceptor. The dansyl moiety is been used as an energy donor because its fluorescence spectrum matches well with the absorption spectrum of rhodamine. The probe shows a reversible ratiometric fluorescent response toward Hg^{2+} with well-resolved emission peaks, a wide linear concentration range, and a fast response time.

Experimental

Reagents and Apparatus

All the chemicals of analytical grade for syntheses were purchased from commercial suppliers and were used without further purification. DMSO of spectroscopic grade and deionized water (distilled) were used throughout the spectroscopic experiment as solvents. Tris–HNO_3 buffer solutions were prepared by using proper amount of Tris and HNO_3 under adjustment by a pH S-3C meter.

NMR spectra were recorded with a 400 MHz Varian spectrometer. Electrospray ionization mass spectra (ESI-MS) were measured on a LC-MSD-Trap-SL instrument. Absorption spectra were obtained on a TU1901 ultraviolet–visible spectrophotometer. The fluorescence spectra were measured with a Cary Eclipse fluorescence spectrometer.

Syntheses

As shown in Scheme 1, compound **1** was synthesized similar to the published procedure [40] by the reaction of compound **2** and dansyl chloride in dichloromethane under the catalysis of triethylamine.

Synthesis of **2**

Compound **2** was prepared similar to the reported procedures by using compound **3** [41] and diethylenetriamine as starting materials [42]. Diethylenetriamine (5 ml, 47 mmol) was added into compound **3** (2.1 g, 3 mmol) in 30 ml absolute ethanol. The mixture was refluxed for 48 h. Then the reaction mixture was allowed to cool to room temperature and the solvent was removed by a rotary evaporator. CH_2Cl_2 (50 mL) and H_2O (50 mL) were added to the residue. After separation, the organic layer was washed with H_2O (50 ml) twice and dried over anhydrous Na_2SO_4 and filtered. The solvent was removed under reduced pressure. 1.2 g of **2** was collected as a brown solid and used for next step without further purification.

Synthesis of **1**

A solution of compound **2** (0.42 g, 0.6 mmol), dansyl chloride (0.201 g, 0.7 mmol) and triethylamine (0.06 g, 0.6 mmol) in 30 mL of dry CH_2Cl_2 was stirred at room temperature for 24 h under N_2. Then the solvent was evaporated *in vacuo*. The residue was purified by column chromatography on silica gel with ethyl acetate/hexanes (1/2, v/v) to afford a white solid of 0.40 g in 72 % yield. ^1H NMR ($CDCl_3$, δ, ppm) 8.51(d, J= 8.4 Hz,1H), 8.32 (d, J=8.8 Hz, 1H), 8.22 (d, J=0.68 Hz, 1H), 7.91–7.93 (m, 1H), 7.53–7.44 (m, 4H), 7.14 (d, J=7.6 Hz, 1H), 7.08–7.06 (m, 3H), 6.15 (s, 2H), 3.11(t, J=6.0 Hz, 8H), 3.08–3.02 (m, 2H), 2.77(s, 6H), 2.76 (t, J=5.6Hz, 2H), 2.36 (t,

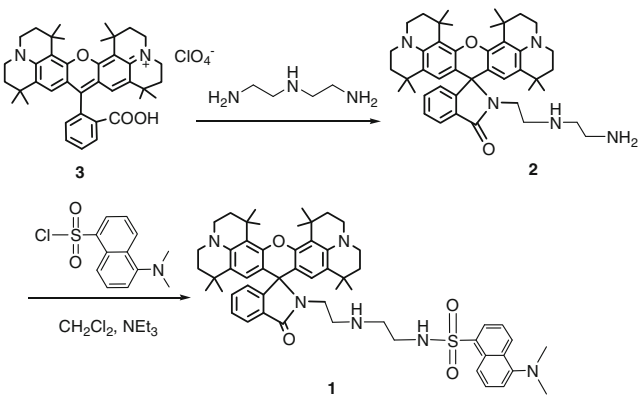

Scheme 1 Synthetic route to compound **1**

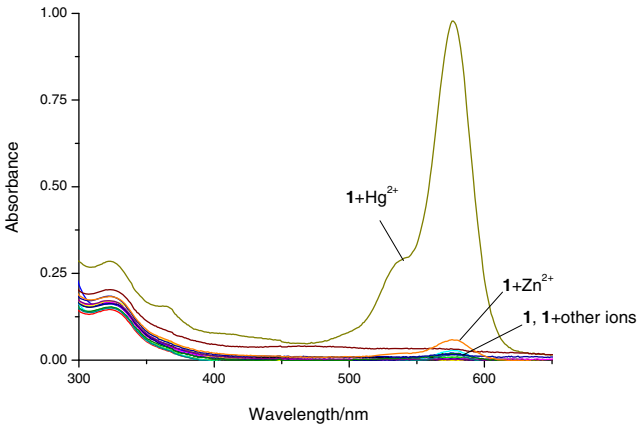

Fig. 1 Absorption spectra of **1** (10 μM) before and after addition of metal ions (30 μM) of nitrate salts of Co^{2+}, Ni^{2+}, Cu^{2+}, Cr^{3+}, Fe^{3+}, Pb^{2+}, Ba^{2+}, Al^{3+}, Ag^{+}, Cd^{2+}, Hg^{2+}, Mn^{2+}, Zn^{2+} and $HgCl_2$

J=6.0 Hz, 2H), 2.09 (d, J=5.6 Hz, 2H), 1.78 (t, J=4.8 Hz, 4H), 1.68 (s, 12H), 1.60 (t, J=6.0 Hz, 6H), 0.97 (s, 6H), 0.88 (s, 6H) (Fig. S1, Supplementary material). ^{13}C NMR (DMSO-d_6, δ, ppm) 167.12, 154.67, 151.78, 150.54, 143.32, 135.99, 134.63, 133.17, 130.34, 130.13, 129.96, 129.66, 129.53, 129.41, 128.91, 128.67, 128.33, 127.22, 123.93, 122.97, 122.50, 119.54, 119.07, 116.50, 115.59, 106.06, 79.64, 72.96, 65.58, 63.54, 48.49, 47.19, 46.13, 45.94, 45.51, 45.44, 41.78, 41.56, 36.33, 32.52, 32.01, 31.39, 30.57, 30.39, 30.28, 29.69, 19.02, 11.83(Fig. S2, Supplementary material). MS (ESI-MS): m/z calculated for $[M]^+$, $C_{56}H_{68}N_6O_4S$, 920.50, found: 921.50 $[M+H]^+$ (Fig. S3, Supplementary material).

Absorption and Fluorescence Experiments

The stock solutions of metal ions (1 mM) were prepared in deionized water from their nitrate salts Co^{2+}, Ni^{2+}, Cu^{2+}, Cr^{3+}, Fe^{3+}, Pb^{2+}, Ba^{2+}, Al^{3+}, Ag^{+}, Cd^{2+}, Hg^{2+}, $Mn^{2+}$and Zn^{2+} of analytical grade. Stock solution of **1** (1 mM) was prepared in DMSO. DMSO-H_2O (4:1, *v/v*) was chosen to dissolve both the organic compound and inorganic salts. In spectral titration experiments, 3 mL solution of **1**, which was diluted to a certain concentration with DMSO-H_2O (4:1, *v/v*), was added into a quartz cell with an optical path length of 1 cm. The stock solution of each metal ion was added into the quartz cell step by step via a syringe. The spectra were recorded at certain minutes after the addition and mixing. For fluorescence measurements, excitation wavelength was provided at 380 nm, and emission was collected from 400 to 700 nm. The excitation slit and emission slit were set at 2.5 and 5 nm respectively.

Results and Discussion

UV/Vis Titration Investigation

The UV-vis spectrum of **1** exhibits a maximum absorbance at 320 nm, which was predominantly due to intraligand π −π*charge transfer (CT) transition. The absence of absorption peak in the visible region demonstrates the existence of **1** in the spirolactam form. The binding ability of **1** in DMSO-H_2O (4:1, *v/v*) was tested with nitrate salts of Co^{2+}, Ni^{2+}, Cu^{2+}, Cr^{3+}, Fe^{3+}, Pb^{2+}, Ba^{2+}, Al^{3+}, Ag^{+}, Cd^{2+}, Hg^{2+}, $Mn^{2+}$and Zn^{2+}. Among these metal ions used, significant changes in absorption spectra of **1** were observed only in the presence of Hg^{2+} (Fig. 1). The UV-vis spectra for **1** (10 μM) with gradual addition of Hg^{2+} in DMSO-H_2O (4:1, *v/v*) have been investigated (Fig. 2a). Upon addition of $Hg(NO_3)_2$ to the solution of **1**, a new absorption band at 577 nm appeared and increased obviously and then increased little (insert in Fig. 2a), with an obvious change in solution color from colorless to bright red, indicating the formation of its ring open amide form and that probe **1** could serve as a 'naked-eye' indicator for Hg^{2+}. The absorbance of **1** at 577 nm increases linearly with the increasing of Hg^{2+} concentration in the range of 0–1.5×10^{-5} mol/L. The relationship between the absorbance at 577 nm and Hg^{2+} concentration was: $A=1.93\times10^{-4}+548.083C$ with a correlation coefficient of $R^2=0.98$ (Fig. 2b), where A was the absorbance at 577 nm and C was

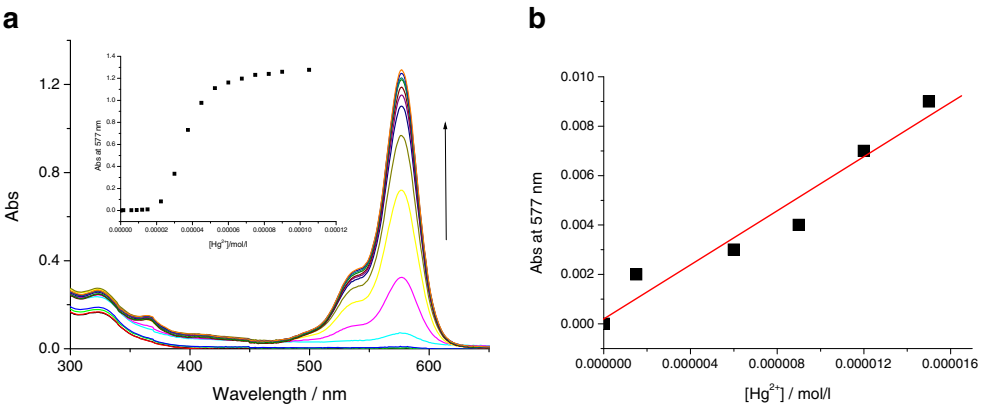

Fig. 2 **a** Absorption spectra of **1** (10 μM) in DMSO-H_2O (4:1, *v/v*) upon addition of Hg^{2+} (insert: Absorbance at 577 nm vs $[Hg^{2+}]$). **b** Linear relationship at low $[Hg^{2+}]$

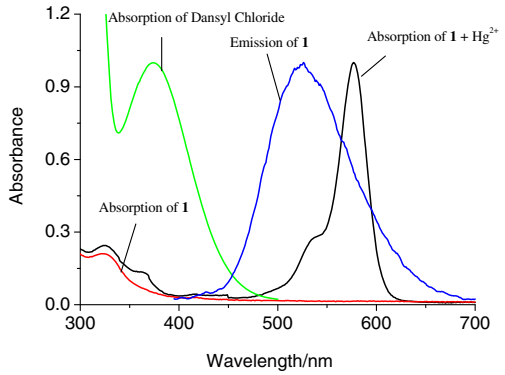

Fig. 3 Absorption spectra of **1** (*red*), **1**+ Hg^{2+} (*black*), dansyl chloride (*green*) and emission spectrum of **1** excited at 380 nm (*blue*)

the concentration of Hg^{2+} in mol/L. At the same time, an absorption shoulder at 370 nm appeared, resulting from dansyl fluorophore, which is confirmed by the absorption spectrum of dansyl chloride (Fig. 3). In compound **1**, dansyl fluorophore was chosen as an energy donor because it has an emission in the visible range and its broad emission (450–650 nm) partially overlaps with the absorption of **1** in the presence of Hg^{2+}, fulfilling a favorable condition for FRET.

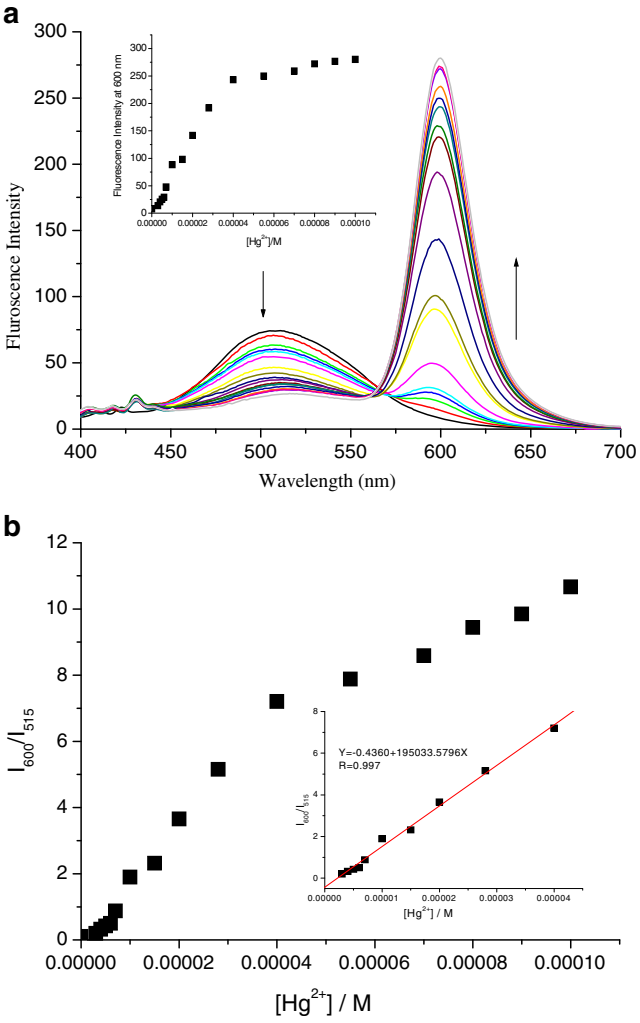

Fig. 4 **a** Fluorescence spectra of **1** (10 μM) in DMSO-H_2O (4:1, *v/v*) upon addition of Hg^{2+}.Insert: Fluorescence intensity at 600 nm vs [Hg^{2+}] **b** I_{600}/I_{515} vs [Hg^{2+}]. Inset: the linear responses at low Hg^{2+} concentrations

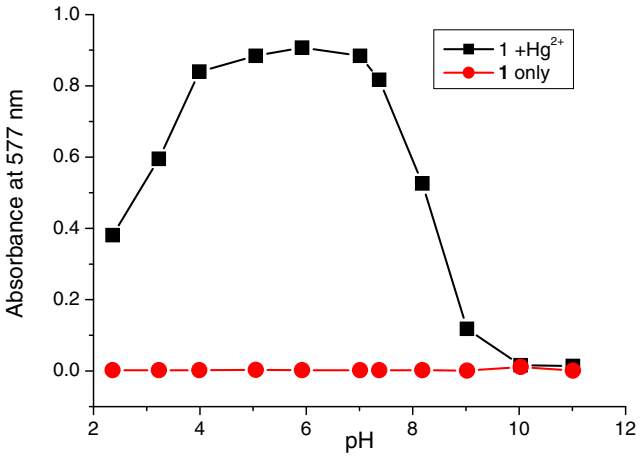

Fig. 5 Absorbance (577 nm) of **1** (10 μM) in 4:1 (*v/v*) DMSO-H_2O (10 mM Tris-HNO_3) with and without Hg^{2+} (50 μM) as a function of pH. **1** (*circle*), **1**+Hg^{2+} (*square*)

The stoichiometry in **1**-Hg^{2+} was studied. Plot of absorbance at 577 nm versus the molar fraction of Hg^{2+} was provided with a total concentration of 1.0×10^{-4} M (Fig. S4, Supplementary material). It was shown that the absorbance went through a maximum at a molar fraction of about 0.5, indicating a 1:1 stoichiometry in the complex **1**-Hg^{2+}. The binding affinity for **1** towards Hg^{2+} was evaluated by spectrophotometric titration. The fitted curve to incorporate the experimental data for Hg^{2+} is shown (Fig. S5, Supplementary material), which gives an association constant *K* value of 2.80×10^{4} M^{-1} for **1** binding to Hg^{2+} [43].

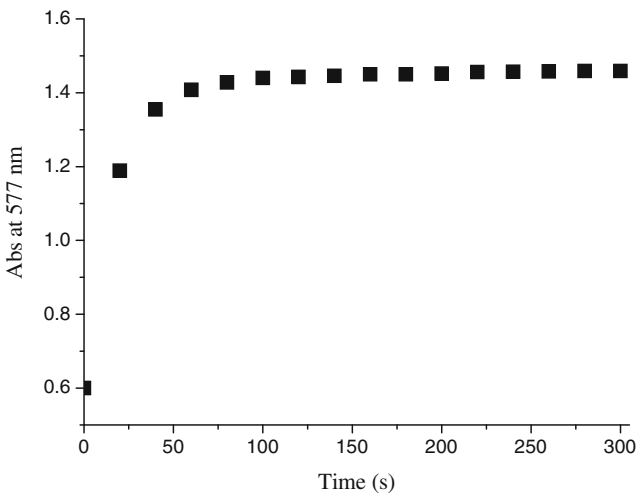

Fig. 6 Kinetics of **1** (10 μM) reaction with Hg^{2+} (100 μM) in DMSO-H_2O (4:1, *v/v*). Absorbance was recorded at 577 nm

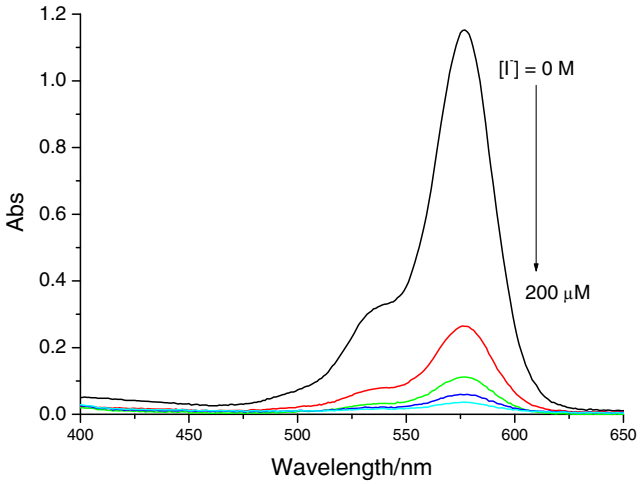

Fig. 7 Absorption spectra of (*from up to down*): **1** (10 μM) with Hg^{2+} (50 μM); addition of KI (50 μM); addition of KI (100 μM); addition of KI (150 μM); addition of KI (200 μM)

Fluorescence Titration Investigation

The fluorescence spectra of **1** in DMSO-H_2O (4:1, *v/v*) containing different concentrations of Hg^{2+} recorded at an excitation wavelength of 380 nm were shown in Fig. 4a. The spectrum of free **1** exhibited only green emission at 515 nm of donor (dansyl) itself, and no characteristic emission of energy acceptor (rhodamine 101 moiety) at 600 nm was observed, indicating that no intramolecular FRET occurred in free **1**. The weak emission of dansyl fluorophore of **1** is probably due to photo-induced electron transfer (PET) from the nitrogen atom of diethylenetriamine moiety that linked with dansyl unit to the photoexcited dansyl moiety. Upon the addition of Hg^{2+}, the donor emission at 515 nm decreased, and a new emission band corresponded to the energy acceptor (rodamine 101 moiety) with a maximum at 600 nm appeared and increased, along with a well-defined isoemissive point at 570 nm, indicating that the configuration transformation of the rhodamine 101 moiety (from the spirocyclic form to a ring-opened amide form) and the subsequent FRET process of **1** are triggered by Hg^{2+}. The ratio of emission intensity of rhodamine 101 and dansyl at 600 and 515 nm I_{600}/I_{515}) varied from 0.11 in the absence of Hg^{2+} to 10.66 when the amount of Hg^{2+} ions reached 9 equiv. of **1**, corresponding to a 97-fold emission ratio increase due to FRET modulation. (Fig. 4b). The response concentration range of **1** for Hg^{2+} covers from 1.0×10^{-6} to 9.0×10^{-5} M (Fig. 4b), with a linear range until 4.0×10^{-5} M (insert in Fig. 4b) with a linear equation: $I=-0.4360+195033.5796C$, $R^2=0.997$ and a detection limit (DL) of 7.7×10^{-8} M (3σ/slope), where σ is the standard deviation of the blank solution; The efficiency of energy transfer (EET) was calculated to be 65 % based on the equation $\eta_{EET}=1-I_{Hg}{}^{2+}/I_0$, where I_0, $I_{Hg}{}^{2+}$ are fluorescence intensities of dansyl moiety at 515 nm in compound **1** (10 μM) in the absence and presence of Hg^{2+} ions (90 μM), respectively [44]. The commonly available $HgCl_2$ failed to induce any change in absorption or fluorescence upon interaction with **1** under identical conditions, possibly due to its higher covalent nature of Hg(II) in $HgCl_2$ and its inability to open the spirolactam form of **1**. This FRET "off–on" sensing system has two distinct advantages. One is the large stokes shift (220 nm) between donor excitation and acceptor emission, which rules out any influence of excitation backscattering effects on fluorescence detection and facilitates the practical application. The other is the presence of two well-separated emission bands with comparable intensities, which ensures accuracy in determining their intensities and ratios.

pH Investigation

The effects of pH on the absorbance of probe **1** (10 μM) in the absence or presence of Hg^{2+} (50 μM) were investigated in a pH range from 2.0 to 11.1 in 4:1 (*v/v*) DMSO-H_2O (10 mM Tris-HNO_3) (Fig. 5). Without Hg^{2+}, no obvious characteristic absorption of rhodamine at 577 nm could be observed for **1** between pH 2.0 and 11.1. Upon addition of Hg^{2+}, the absorbance at 577 nm increased dramatically when the pH value was between 4.0 and 8.2, indicating that Hg^{2+} detection could be carried out in weak acidic till weak base conditions.

Response Time and Reversibility Investigation

The time dependence of the response of **1** to Hg^{2+} was investigated by recording the change of absorbance at 577 nm with

Scheme 2 Proposed mechanism for FRET of **1** with Hg^{2+}

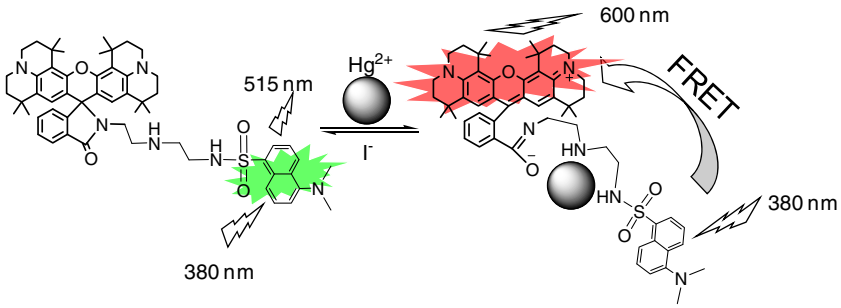

time (Fig. 6). The results revealed that the reaction of compound **1** (10 μM) and Hg^{2+} (100 μM) was completed within 1 min, indicating that chemosensor **1** could meet the response time requirements for real-time monitoring of Hg^{2+} in practical samples.

The reversibility of the binding process between **1** and Hg^{2+} was established when the original spectrum for **1** was restored upon addition of KI to the solution of **1**-Hg^{2+} in DMSO-H_2O (4:1, *v/v*). I^- ions have a strong affinity for Hg^{2+}, and its binding constant is much higher than that for **1**. This caused demetalation of **1**-Hg^{2+} to HgI_2 or $[HgI_4]^{2-}$ and regeneration of the spirolactam ring with the disappearance of the absorption band at 577 nm (Fig. 7). The addition of bidentate ligand ethylenediamine to **1**-Hg^{2+} could also decrease the absorption at 577 nm (Fig. S6, supplementary material). Thus the sensing process of **1** to Hg^{2+} was considered to be reversible rather than an ion-catalyzed hydrolysis reaction. The proposed binding mechanism of Hg^{2+} with **1** was shown in Scheme 2. The carbonyl O, imino N, and the other two N atoms in the linker diethylenetriamine of **1** are the most possible binding sites for Hg^{2+}.

Selectivity Investigation

Changes of fluorescence spectra of **1** caused by Fe^{3+}, Al^{3+}, Ba^{2+}, Co^{2+}, Ni^{2+}, Cu^{2+}, Pb^{2+}, Cd^{2+}, Ag^+, Mn^{2+}, Hg^{2+}, Zn^{2+} and Cr^{3+} in DMSO-H_2O (4:1, *v/v*) are recorded (Fig. S7, Supplementary material). The competitive cations did not lead to any significant fluorescence spectra changes of **1** except for Hg^{2+}. Coexisting ions of Fe^{3+}, Al^{3+}, Ba^{2+}, Co^{2+}, Ni^{2+}, Cu^{2+}, Pb^{2+}, Cd^{2+}, Ag^+, Mn^{2+}, $Cr^{3+}$and Zn^{2+} have negligible effects on the ratiometric fluorescence detection of Hg^{2+} (Fig. 8). These results suggest that **1** could be used as an Hg^{2+} selective fluorescent chemosensor in the presence of competing metal ions, especially Cu^{2+}, Fe^{3+}, Zn^{2+} and Pb^{2+}, which are known to be important competitors.

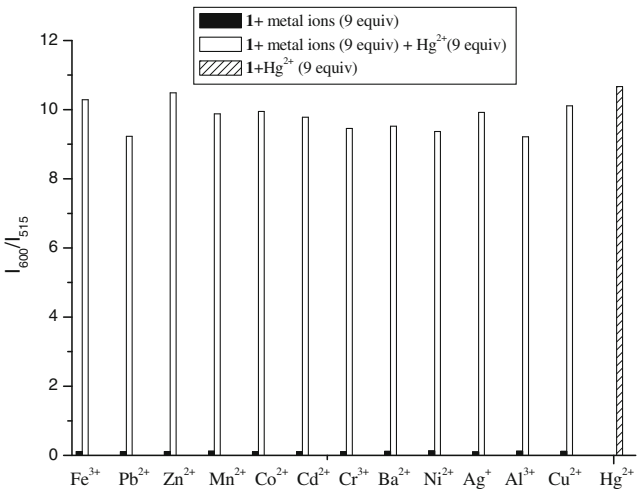

Fig. 8 I_{600}/I_{515} for **1** (10 μM) in the presence of different metal ions (90 μM), and upon further addition of Hg^{2+} (90 μM)

Conclusions

We have developed a novel FRET fluorescent sensor based on the spirolactam form of rhodamine 101 linked with dansyl by diethylenetriamine. It exhibits a clear Hg^{2+} induced change in the intensity ratio of the two well-separated emission band of dansyl unit and rhodamine 101. The dansyl moiety serves as the energy donor, and a very efficient ring-opening reaction induced by Hg^{2+} generates the long-wavelength rhodamine101 fluorophore that can act as the energy acceptor. The FRET processes were found to be fast, reversible and selective in the red spectral region. This strategy provides a ratiometric fluorescent sensor for Hg^{2+}, allowing for a large stokes shift (220 nm) between donor excitation and acceptor emission, which rules out any influence of excitation backscattering effects on fluorescence detection.

Acknowledgments The authors thank the NSFC (project No. 21102037) and the Education Department of Henan Province (No. 2010GGJS-048) for the financial support.

References

1. Zhao Q, Li F, Huang C (2010) Phosphorescent chemosensors based on heavy-metal complexes. Chem Soc Rev 39:3007–3030
2. Tsukanov AV, Dubonosov AD, Bren VA, Minkin VI (2008) Organic chemosensors with crown-ether groups (review). Chem Heterocycl Compd 44:899–923
3. Prodi L, Balletta F, Mantalti M, Zaccheroni N (2000) Luminescent chemosensors for transition metal ions. Coord Chem Rev 205:59–83
4. Chen X, Pradhan T, Wang F, Kim JS, Yoon J (2012) Fluorescent chemosensors based on spiroring-opening of xanthenes and related derivatives. Chem Rev 112:1910–1956
5. Boening DW (2000) Ecological effects, transport, and fate of mercury: a general review. Chemosphere 40:1335–1351
6. Renzoni A, Zino F, Franchi E (1998) Mercury levels along the food chain and risk for exposed populations. Environ Res 77:68–72
7. Zhang D, Su JH, Ma X, Tian H (2008) An efficient multiple-mode molecular logic system for pH, solvent polarity, and Hg^{2+} ions. Tetrahedron 64:8515–8521
8. Zalups RK, Lash LH (2006) Cystine alters the renal and hepatic disposition of inorganic mercury and plasma thiol status. Toxicol Appl Pharmacol 214:88–97
9. Zalups RK, Ahmad S (2004) Homocysteine and the renal epithelial transport and toxicity of inorganic mercury: role of basolateral transporter organic anion transporter 1. J Am Soc Nephrol 15:2023–2031
10. Silbergeld EK, Silva IA, Nyland JF (2005) Mercury and autoimmunity: implications for occupational and environmental health. Toxicol Appl Pharmacol 207:s282–s292
11. de Silva AP, Gunaratne HQN, Gunnlaugsson T, Huxley AJM, McCoy CP, Rademacher JT, Rice TE (1997) Signaling recognition events with fluorescent sensors and switches. Chem Rev 97:1515–1566

12. Chen X, Tian X, Shin I, Yoon J (2011) Fluorescent and luminescent probes for detection of reactive oxygen and nitrogen species. Chem Soc Rev 40:4783–4804
13. Czarnik AW (1993) Fluorescent chemosensors for ion and molecule recognition. American Chemical Society, Washington
14. Banerjee T, Suresh M, Ghosh HN, Das A (2011) Eur J Inorg Chem 30:4680–4690
15. Rurack K (2001) Flipping the light switch 'ON' - the design of sensor molecules that show cation-induced fluorescence enhancement with heavy and transition metal ions. Spectrochim Acta A 57:2161–2195
16. Suresh M, Shrivastav A, Mishra S, Suresh E, Das A (2008) A rhodamine-based chemosensor that works in the biological system. Org Lett 10:3013–3016
17. Kim HN, Nam S-W, Swamy KMK, Jin Y, Chen X, Kim Y, Kim S-J, Park S, Yoon J (2011) Rhodamine hydrazone derivatives as Hg^{2+} selective fluorescent and colorimetric chemosensors and their applications to bioimaging and microfluidic system. Analyst 136:1339–1343
18. Huang W, Zhou P, Yan W, He C, Xiong L, Li F, Duan C (2009) A bright water-compatible sugar-rhodamine fluorescence sensor for selective detection of Hg^{2+} in natural water and living cells. J Environ Monit 11:330–335
19. Tang L, Li F, Liu M, Nandhakumar R (2011) Single sensor for two metal ions: colorimetric recognition of Cu^{2+} and fluorescent recognition of Hg^{2+}. Spectrochim Acta A 78:1168–1172
20. Wu D, Huang W, Duan C, Lin Z, Meng Q (2007) Highly sensitive fluorescent probe for selective detection of Hg^{2+} in DMF aqueous media. Inorg Chem 46:1538–1540
21. Wu D, Huang W, Lin Z, Duan C, He C, Wu S, Wang D (2008) Highly sensitive multiresponsive chemosensor for selective detection of Hg^{2+} in natural water and different monitoring environments. Inorg Chem 47:7190–7201
22. Huang W, Wu D-Y, Duan C-Y (2010) Conformation-switched chemosensor for selective detection of Hg^{2+} in aqueous media. Inorg Chem Commun 13:294–297
23. Yang H, Zhou Z, Huang K, Yu M, Li F, Yi T, Huang C (2007) Multisignaling optical-electrochemical sensor for Hg^{2+} based on a rhodamine derivative with a ferrocene unit. Org Lett 9:4729–4732
24. Du J, Fan J, Peng X, Sun P, Wang J, Li H, Sun S (2010) A new fluorescent Chemodosimeter for Hg^{2+}: selectivity, sensitivity, and resistance to Cys and GSH. Org Lett 12:476–479
25. Shiraishi Y, Sumiya S, Kohno Y, Hirai T (2008) A rhodamine-cyclen conjugate as a highly sensitive and selective fluorescent chemosensor for Hg(II). J Org Chem 73:8571–8574
26. Kwon SK, Kim HN, Rho JH, Swamy KMK, Shanthakumar SM, Yoon J (2009) Rhodamine derivative bearing histidine binding site as a fluorescent chemosensor for Hg^{2+}. Bull Korean Chem Soc 30:719–721
27. Tsien RY, Poenie M (1986) Fluorescence ratio imaging: a new window into intracellular ionic signaling. Trends Biochem Sci 11:450–455
28. Guliyev R, Coskun A, Akkaya EU (2009) Design strategies for ratiometric chemosensors: modulation of excitation energy transfer at the energy donor site. J Am Chem Soc 131:9007–9013
29. Zhou Z, Yu M, Yang H, Huang K, Li F, Yi T, Huang C (2008) FRET-based sensor for imaging chromium(III) in living cells. Chem Commun 3387–3389
30. Shang G-Q, Gao X, Chen M-X, Zheng H, Xu J-G (2008) A novel Hg^{2+} selective ratiometric fluorescent chemodosimeter based on an intramolecular FRET mechanism. J Fluoresc 18(6):1187–1192
31. Lee MH, Kim HJ, Yoon S, Park N, Kim JS (2008) Metal ion induced FRET OFF-ON in Tren/Dansyl-appended rhodamine. Org Lett 10:213–216
32. Tolosa L, Nowaczyk K, Lakowicz J (2002) In an introduction to laser spectroscopy. In: Fluorescence for biochemical systems, 2nd ed. Kluwer Academic/Plenum Publishers, New York
33. Zhang X, Xiao Y, Qian X (2008) A ratiometric fluorescent probe based on FRET for imaging Hg^{2+} ions in living cells. Angew Chem Int Ed 47(42):8025–8029
34. Othman AB, Lee JW, Wu JS, Kim JS, Abidi R, Thuery P, Strub JM, Dorsselaer AV, Vicens J (2007) Calix[4]arene-based, Hg^{2+} -induced intramolecular fluorescence resonance energy transfer chemosensor. J Org Chem 72:7634–7640
35. Yuan MJ, Zhou WD, Liu XF, Zhu M, Li JB, Yin XD, Zheng HY, Zuo ZC, Ouyang CB, Liu HB, Li YL, Zhu DB (2008) A multianalyte chemosensor on a single molecule: promising structure for an integrated logic gate. J Org Chem 73:5008–5014
36. Lee YH, Lee MH, Zhang JF, Kim JS (2010) Pyrene excimer-based Calix[4]arene FRET chemosensor for mercury(II). J Org Chem 75:7159–7165
37. Yu HB, Xiao Y, Guo HY, Qian XH (2011) Convenient and efficient FRET platform featuring a rigid biphenyl spacer between rhodamine and BODIPY: transformation of Turn-On' sensors into ratiometric ones with dual emission. Chem Eur J 17:3179–3191
38. Fang G, Xu MY, Zeng F, Wu SZ (2010) β-Cyclodextrin as the vehicle for forming ratiometric mercury ion sensor usable in aq. media, biol. fluids, and live cells. Langmuir 26:17764–17771
39. Zhou Z, Li Y, Wu Y (2014) Ratiometric fluorescence probe for two-photon bioimaging of Cr^{3+} in living cells. Tetrahedron Lett 55(30):4075–4077
40. Xie P, Guo F, Xia R, Wang Y, Yao D, Yang G, Xie L (2014) A rhodamine–dansyl conjugate as a FRET based sensor for Fe^{3+} in the red spectral region. J Lumin 145:849–854
41. Uddin Md J, Marnett LJ (2008) Synthesis of 5- and 6-carboxy-X-rhodamines. Org Lett 10:4799–4801
42. Zhang X, Shiraishi Y, Hirai T (2007) Cu(II)-selective green fluorescence of a rhodamine−diacetic acid conjugate. Org Lett 9:5039–5042
43. Zhao Y, Zhang X-B, Han Z-X, Qiao L, Li C-Y, Jian L-X, Shen G-L, Yu R-Q (2009) A highly sensitive and selective colorimetric and off-on fluorescent chemosensor for Cu^{2+} in aqueous solution and living cells. Anal Chem 81:7022–7030
44. Liu B, Zeng F, Wu G, Wu S (2011) A FRET-based ratiometric sensor for mercury ions in water with multi-layered silica nanoparticles as the scaffold. Chem Commun 47:8913–8915